

Performance Analysis of Synergetic UAV-RIS Communication Networks

1

Dimitrios Tyrovolas, *Student Member, IEEE*, Sotiris A. Tegos, *Student Member, IEEE*, Panagiotis D. Diamantoulakis, *Senior Member, IEEE*, and George K. Karagiannidis, *Fellow, IEEE*

Abstract—The effective integration of unmanned aerial vehicles (UAVs) in future wireless communication systems depends on the conscious use of their limited energy, which constrains their flight time. Reconfigurable intelligent surfaces (RISs) can be used in combination with UAVs with the aim to improve the communication performance without increasing complexity at the UAVs’ side. In this paper, we propose a synergetic UAV-RIS communication system, utilizing a UAV with a directional antenna aiming to the RIS. Also, we present the link budget analysis and closed-form expressions for the outage probability as well as for an important second order statistical parameter of the proposed synergetic UAV-RIS communication system, the average outage duration. Finally, numerical results illustrate the effectiveness of the proposed synergetic system.

Index Terms—Reconfigurable intelligent surfaces, UAV, link budget analysis, outage probability, average outage duration

I. INTRODUCTION

One of the major requirements for future wireless communication networks is the effective integration of unmanned aerial vehicles (UAVs) [1]. UAVs are envisioned to be used in a twofold way, i.e., either as i) mobile equipment for a vast number of operations including sensing and monitoring or ii) as part of the network’s infrastructure for coverage extension, traffic offloading in crowded environments, and rapid recovery of the network services in cases of emergency. In both use cases, the effective utilization of UAVs depends on mainly two interrelated factors, the communication performance, e.g., in terms of data rate, reliability, and latency, as well as the UAVs’ flight time duration which is limited by their battery capacity. Thus, it becomes of paramount importance to increase the communication quality-of-service (QoS), without increasing the energy consumption at the UAVs.

To this end, UAVs can be used in combination with reconfigurable intelligent surfaces (RISs), which can facilitate the signal beamforming through elements that can shift the phase of the reflected signals [2], without increasing complexity at the UAVs’ side. Similar scenarios have been studied in [3] where the joint UAV trajectory and RIS’s passive beamforming design is investigated in order to maximize the average achievable rate. More specifically, the authors in [3] used an omnidirectional antenna for the UAV which results in increased beam waste. Considering though that a RIS will be a stable target with non-negligible dimensions and high beamforming capabilities, UAVs can directly transmit towards the RIS in order to avoid applying complex signal processing algorithms for beamforming and not waste any power due to

The authors are with the Wireless Communications and Information Processing (WCIP) Group, Electrical & Computer Engineering Dept., Aristotle University of Thessaloniki, 54 124, Thessaloniki, Greece (e-mails: {tyrovolas,tegosoti,padiaman,geokarag}@auth.gr).

omnidirectional transmission. However, this scenario has not been investigated in the existing literature.

Existing link budget models do not adequately describe the losses in the aforementioned scenario. For example, although the losses in RIS-aided communication systems in highly-directional millimeter wave links were partially investigated in [4], the derived results may be proven inaccurate in UAV communication scenarios where the UAV can be arbitrarily located in the three-dimensional (3D) space. This is due to the fact that the proposed model in [4] is based on the assumptions that the radiation footprint and the RIS axes and center always coincide and either the radiation footprint or the RIS is a subarea of each other. Moreover, to fully investigate the potential of using UAVs and RISs in a synergetic way, except of the outage probability (OP), the temporal variations of the outage also need to be taken into account. These variations are characterized by the average outage duration (AOD), which is a second order statistics metric, also known as average fade duration. The AOD is of paramount importance for all communication systems and especially for ultra-reliable low latency communications (URLLC), because it facilitates the Markov modeling of wireless channels and determines the optimal packet length as well as the packet error rate [5]. Nevertheless, to the best of the authors’ knowledge, the investigation of second order statistics has never been attempted in the context of RIS-assisted communication systems.

To address the aforementioned issues, in this paper, a synergetic UAV-RIS communication system is proposed and its performance is analyzed, utilizing a UAV with a directional antenna aiming to the RIS. More specifically, we provide a link budget analysis, deriving the average received signal to noise ratio (SNR) as a function of the node’s position in the 3D space. Moreover, we derive closed-form expressions for both the OP and the AOD. Furthermore, we provide numerical results which illustrate the performance of the proposed system for different scenarios regarding the node’s positions. Among others, the impact the distance on the average received SNR and boundaries of the area where the UAV is permitted to hover into in order to ensure that the AOD is lower than a predefined threshold are illustrated.

II. SYSTEM MODEL

We consider a communication network consisting of a UAV, a RIS and a ground node (GN) equipped with a single omnidirectional antenna. The UAV-RIS and RIS-GN links are established and constitute an alternative path to the direct UAV-GN link which is assumed to be blocked. Since the RIS has significant dimensions, in order to exploit its beamforming capabilities, the UAV is equipped with a directional antenna

which is steered towards the RIS. Furthermore, the UAV is located at an arbitrary point (r, θ, ϕ) , where r is the UAV-RIS center distance, $\theta \in [0, \pi]$ is the elevation angle and $\phi \in [0, \pi]$ is the azimuth angle. Moreover, the RIS is placed onto the plane $y = 0$ and it is assumed that the UAV always aims to a proper point K in order the radiation footprint's center to coincide with the RIS center C , which is considered as the origin of the axes, as illustrated in Fig. 1. The points B and D are the projection of the UAV on the plane $z = 0$ and the projection of B on the x axis, respectively. In addition, ϕ' can be defined similarly to ϕ by replacing C with K . Also, the antenna's three-dimensional radiation pattern can be considered as a cone with fixed spreading angle ξ [4]. According to the conic-section theory, the section of a cone and a rectangular plane is either a circle or an ellipse, thus the footprint upon the RIS plane is also a circle or an ellipse [6]. The transmitted signal from the UAV antenna impinges upon the RIS which consists of N reflecting elements and then it is reflected towards the GN.

The RIS acts as a passive beamformer which adjusts the elements' reflection coefficient phase and shapes the transmitted signal in a desired way. However, as the transmission is directional, the number of illuminated elements M may be different from N . Thus, the received signal at the GN, Y , can be expressed as

$$Y = \sqrt{l_0 G P_t} \sum_{i=1}^M |H_{i1}| |H_{i2}| e^{-j(\omega_i + \arg(H_{i1}) + \arg(H_{i2}))} X + W, \quad (1)$$

where X is the transmitted signal for which it is assumed that $\mathbb{E}[|X|^2] = 1$ with $\mathbb{E}[\cdot]$ and $\arg(\cdot)$ denoting expectation and the argument of a complex number, respectively. Also, P_t denotes the transmit power, $G = G_t G_r$ is the product of the UAV and the GN antenna gains, and H_{i1} and H_{i2} are the complex channel coefficients that correspond to the i -th UAV-RIS and RIS-GN link, respectively. Moreover, W is the additive white Gaussian noise, ω_i is the phase correction term, and $l_0 = l_1 l_2$ with l_1 and l_2 being the path losses that correspond to the UAV-RIS and RIS-GN links, respectively. More specifically, l_1 equals to the fraction of the reflecting element's effective aperture to the radiation footprint area and l_2 can be modeled as [7]

$$l_2 = C_0 \left(\frac{d_u}{d_0} \right)^{-n}. \quad (2)$$

In (2), C_0 denotes the reference path loss at the reference distance d_0 , d_u denotes the distance of the RIS-GN link and n expresses the path loss exponent.

Furthermore, it should be highlighted that due to the UAV's directional antenna and the UAV-RIS channel's nature which corresponds to an air to air channel, there is no fading in the UAV-RIS link, thus $|H_{i1}| = 1$ and $\arg(H_{i1}) = \frac{2\pi r}{\lambda}$ with λ being the carrier's frequency wavelength. Additionally, it is assumed that $|H_{i2}|$ is a random variable (RV) following the Nakagami- m distribution with shape parameter m and spread parameter Ω . Also, the RIS adjusts the phase correction term to cancel the overall phase shift, i.e., $\omega_i = -\frac{2\pi r}{\lambda} - \arg(H_{i2})$.

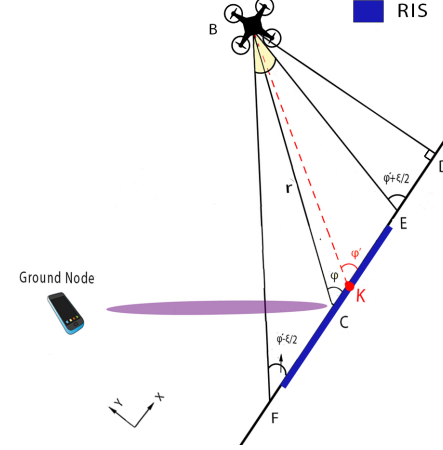


Fig. 1. The UAV-RIS synergetic communication system's layout.

Thus, the received signal at the GN can be rewritten as

$$Y = \sqrt{l_0 G P_t} H X + W, \quad (3)$$

where

$$H = \sum_{i=1}^M |H_{i2}|. \quad (4)$$

III. PERFORMANCE ANALYSIS

In this section, we present the average received SNR, the OP and the AOD for the proposed synergetic UAV-RIS system.

A. Link Budget Analysis

The instantaneous received SNR at the GN is given by

$$\gamma_r = l_0 G \gamma_t |H|^2, \quad (5)$$

where $\gamma_t = \frac{P_t}{\sigma^2}$ is the transmit SNR and σ^2 denotes the noise power. In (5), we need to determine the path loss l_0 of the proposed synergetic system and to investigate the channel gain through the calculation of the number of the illuminated elements. To this end, we first define

$$g(x) = \left| \frac{r \sin(\phi) \sin(\theta)}{\tan(\phi)} - \frac{r \sin(\phi) \sin(\theta)}{\tan(x + \frac{\xi}{2})} \right| - \left| \frac{r \sin(\phi) \sin(\theta)}{\tan(x - \frac{\xi}{2})} - \frac{r \sin(\phi) \sin(\theta)}{\tan(\phi)} \right|, \quad (6)$$

where $x \in [\phi, \frac{\pi}{2}]$ if $\phi \leq \frac{\pi}{2}$ and $x \in (\frac{\pi}{2}, \phi]$ if $\phi > \frac{\pi}{2}$.

In the following proposition, we provide the path loss of the link between the UAV and the RIS.

Proposition 1: The path loss of the UAV-RIS link can be expressed as

$$l_1 = \frac{A}{\pi r^2} \left(\left| \frac{\sin(\phi) \sin(\theta)}{\tan(\phi)} - \frac{\sin(\phi) \sin(\theta)}{\tan\left(\phi' + \frac{\xi}{2}\right)} \right| \tan\left(\frac{\xi}{2}\right) \right)^{-1}, \quad (7)$$

where A denotes the effective aperture of the reflecting element which equals to its area and ϕ' can be calculated with numerical methods as the root of $q(\phi') = 0$.

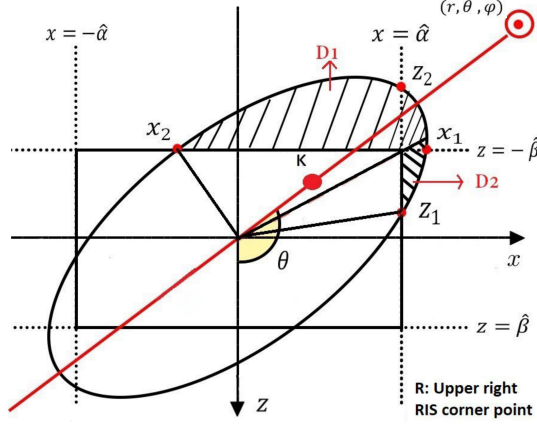


Fig. 2. Radiation footprint at plane $y = 0$ and UAV's location at plane $y = r \sin(\theta) \sin(\phi)$.

Proof: See Appendix A. ■

After the calculation of the footprint area, considering the position of the UAV, there can be five cases regarding the radiation footprint and its intersection points with the RIS sides. It should be highlighted that only the areas D_1 and D_2 , which are illustrated in Fig. 2, need to be calculated due to the geometrical problem's symmetry. Considering that x_1, x_2 and z_1, z_2 are the intersection point pairs of the footprint with the lines that define the upper and the right RIS sides, respectively, as shown in Fig. 2, the cases are the following:

- C_1 : No intersection points exist, i.e., the footprint is inside the RIS, thus no spillover losses exist.
- C_2 : Intersection points k_1, k_2 exist only in one RIS side where $k \in \{x, z\}$.
- C_3 : All intersection points exist and are on the RIS sides.
- C_4 : All intersection points exist and only one of each pair lies on the RIS side.
- C_5 : All intersection points exist and are beyond the RIS sides, i.e., the RIS is inside the footprint, thus all the reflecting elements are being illuminated.

By taking into account the aforementioned cases, in the following proposition we provide the number of illuminated reflecting elements as well as the spillover losses which correspond to the radiation footprint parts that lay outside of the RIS to calculate the average channel gain of the proposed synergetic system. To this end, we first define $E_{QV} = \frac{(t_2-t_1)\alpha(\xi)\beta(\xi)}{2}$ which expresses the area of an elliptic arc which is defined by the origin and two points $Q \equiv (m_1, n_1)$ and $V \equiv (m_2, n_2)$, where V is located counter-clockwise related to Q [8]. Moreover, t_1 is the angle that is shaped with the major axis and the line that connects the origin with Q and t_2 is the angle that is shaped similarly with V . These angles can be calculated as in Table 1 in [8]. Finally, $T_{QV} = \frac{|m_1n_2 - m_2n_1|}{2}$ denotes a triangle area whose vertex coincides with the origin and base is formed from the points $Q \equiv (m_1, n_1)$ and $V \equiv (m_2, n_2)$ [8].

Proposition 2: The channel coefficient H can be approximated with \tilde{H} which follows the normal distribution with parameters $\mathbb{E}[\tilde{H}] = M \frac{\Gamma(m+\frac{1}{2})}{\Gamma(m)} \left(\frac{\Omega}{m}\right)^{\frac{1}{2}}$ and $\text{Var}[\tilde{H}] =$

$M\Omega \left(1 - \frac{1}{m} \left(\frac{\Gamma(m+\frac{1}{2})}{\Gamma(m)}\right)^2\right)$, where $\Gamma(\cdot)$ is the gamma function and

$$M = \left\lfloor \frac{E_f (1 - J)}{4\hat{\alpha}\hat{\beta}} N \right\rfloor \quad (8)$$

with

$$J = \begin{cases} 0, & \text{if } C_1 \\ \frac{2(E_{k_1 k_2} - T_{k_1 k_2})}{E_f}, & \text{if } C_2 \\ \frac{2(E_{x_1 x_2} - T_{x_1 x_2} + E_{z_1 z_2} - T_{z_1 z_2})}{E_f}, & \text{if } C_3 \\ \frac{2(E_{z_1 x_2} - T_{R x_2} - T_{z_1 R})}{E_f}, & \text{if } C_4 \\ 1 - \frac{4\hat{\alpha}\hat{\beta}}{E_f}, & \text{if } C_5 \end{cases} \quad (9)$$

denoting the percentage of the footprint area which is lost due to spillover losses and $\lfloor \cdot \rfloor$ being the floor operator. ■

Proof: See Appendix B. ■

Remark 1: Considering that \tilde{H} follows the normal distribution, $|\tilde{H}|^2$ is a RV following the non-central chi-square distribution with one degree of freedom and non centrality parameter equal to $\mathbb{E}^2[\tilde{H}]$, thus

$$\mathbb{E}[|\tilde{H}|^2] = \left(\frac{\Omega}{m}\right) \left(M \frac{\Gamma(m+\frac{1}{2})}{\Gamma(m)}\right)^2 + 1. \quad (10)$$

Therefore, the average received SNR can be calculated as

$$\mathbb{E}[\gamma_r] = l_0 G \gamma_t \mathbb{E}[|\tilde{H}|^2]. \quad (11)$$

B. Outage Probability and Average Outage Duration

Next, we derive the OP, which is defined as the probability that the instantaneous received SNR is below a specified threshold, in order to evaluate the considered system's reliability. To this end, we set the parameter $z = \sqrt{\frac{\gamma_{\text{thr}}}{l_0 G \gamma_t}}$, where γ_{thr} is the outage threshold value of the received SNR.

Corollary 1: The OP can be obtained as

$$\mathcal{P}_o(z) = \frac{1}{2} \left[1 + \text{erf} \left(\frac{z - M \frac{\Gamma(m+\frac{1}{2})}{\Gamma(m)} \left(\frac{\Omega}{m}\right)^{\frac{1}{2}}}{\sqrt{2} M \Omega \left(1 - \frac{1}{m} \left(\frac{\Gamma(m+\frac{1}{2})}{\Gamma(m)}\right)^2\right)} \right) \right], \quad (12)$$

where $\text{erf}(\cdot)$ is the error function,

Proof: The OP is defined as

$$\mathcal{P}_o(z) = \Pr(\gamma_r \leq \gamma_{\text{thr}}) = \Pr(H \leq z). \quad (13)$$

Considering the approximation \tilde{H} which follows the normal distribution, we can calculate the OP through the cumulative density function and derive (12) which completes the proof. ■

In the following corollary, we provide the AOD which is defined as the average time that the fading envelope remains below a specified level after crossing that level in a downward direction and characterizes the temporal variation of the outage probability and is closely related to the system's delay. The AOD is calculated as the fraction of the outage probability at a threshold z to the level crossing rate (LCR) at z which is

defined as the rate at which the received signal crosses the threshold z in the negative direction.

Corollary 2: The AOD can be calculated as

$$A(z) = \frac{2\mathcal{P}_o(z)\sqrt{m\text{Var}[\tilde{H}]}}{e^{-\frac{(z-\mathbb{E}[\tilde{H}])^2}{2\text{Var}[\tilde{H}]}} f_D \sqrt{M\Omega}}, \quad (14)$$

where f_D is the maximum Doppler spread. \blacksquare

Proof: See Appendix C.

IV. SIMULATION RESULTS

In this section, we illustrate the performance of the proposed synergistic UAV-RIS system. We examine two communication scenarios which correspond to a LoS and a non-LoS (nLoS) scenario between the RIS and the GN, where we set the shape parameter of the second link $m = 3$ for the first scenario and $m = 1$ for the second one and the spreading parameter $\Omega = 1$ for both cases. For the second link, we set $C_0 = -30$ dB, $d_0 = 1$ m, $d_u = 50$ m and the path loss exponent $n = 2.2$ for both scenarios. Furthermore, we set the transmit SNR $\gamma_t = 70$ dB, the threshold value $\gamma_{\text{thr}} = 20$ dB and the UAV's antenna spreading angle $\xi = 15^\circ$. Moreover, we set the RIS dimensions as $2\hat{\alpha} = 2$ m and $2\hat{\beta} = 1$ m, the number of the reflecting elements $N = 800$, the carrier's frequency is equal to 3 GHz and each element's area $A = \frac{\lambda^2}{4}$. It should be mentioned that the inter-distance between the elements is assumed to be 0 and the mutual coupling between the reflecting elements is neglected. Finally, we calculate the UAV's antenna gain as $G_t = \frac{29000}{\theta^2}$ [9], and considering that the GN antenna is omnidirectional, we set $G_r = 1$.

Fig. 3 illustrates the impact of the UAV-RIS distance to the average received SNR. As the distance increases, the average received SNR starts to increase due to the fact that more reflecting elements are being illuminated. However, after a certain distance the average received SNR starts to increase slower due to spillover losses. The reason why the average received SNR continues to increase is due to the fact that the illuminated elements keep increasing as the UAV moves away from the RIS. When all the elements are illuminated, the spillover losses continue to increase as the distance r increases leading to rapid decrease of the average received SNR.

Fig. 4 depicts how the OP is affected from the UAV-RIS distance. It can be observed that if $m = 3$ and $\theta = \frac{\pi}{2}$, i.e., the UAV is at the level of the RIS center, the UAV can ensure low OP for distances up to 240 m. Thus, Fig. 4 demonstrates that the cooperation of UAVs equipped with directional antennas and RIS can potentially provide ultra reliable communications.

In Fig. 5, we illustrate the area boundaries where the UAV is permitted to hover into, in order to ensure that the AOD, is less than 1 ms. The maximum Doppler spread is set at 10 Hz. As θ diverges from $\frac{\pi}{2}$ or the required AOD value decreases, the area that the UAV can hover into also decreases. Moreover the fading conditions of the RIS-GN link can also affect the AOD. Thus, in order to keep the AOD value low, the RIS should be placed properly in order to ensure good fading conditions between the RIS and the GN.

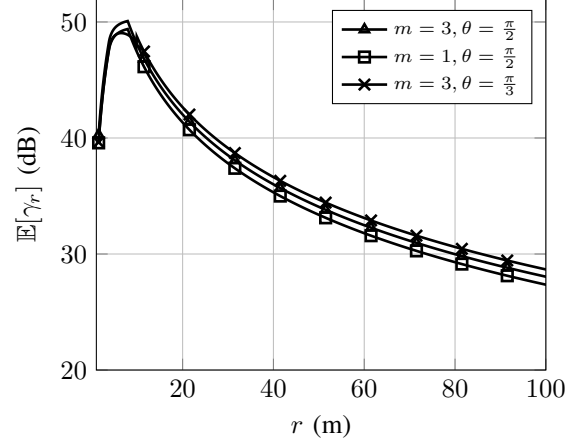


Fig. 3. Average received SNR versus UAV-RIS distance r .

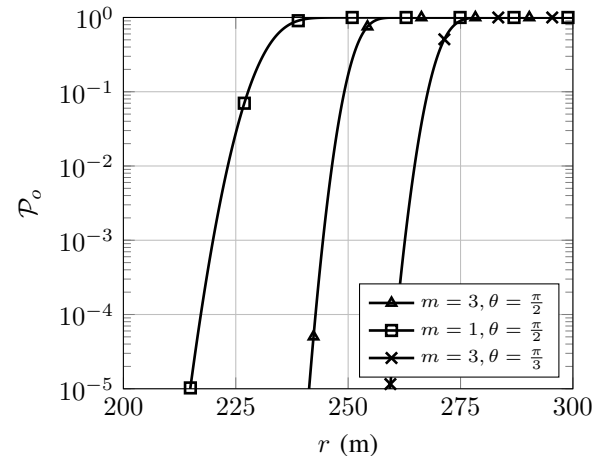


Fig. 4. OP versus UAV-RIS distance r .

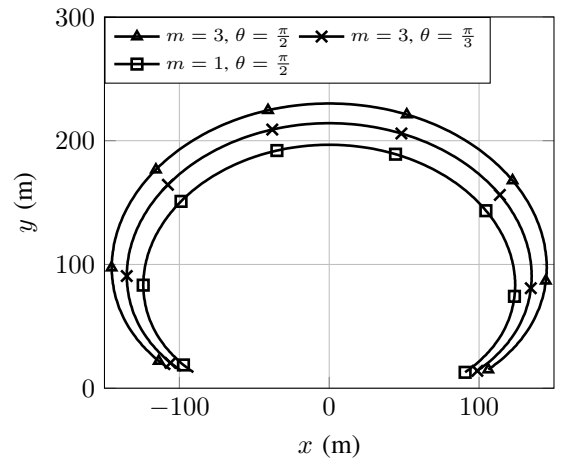


Fig. 5. Hovering permitted area boundaries for AOD = 1 ms.

V. CONCLUSIONS

In this work, we have proposed a synergetic UAV-RIS system where a UAV equipped with a directional antenna acts as an aerial communication node that serves a GN with the aid of a RIS. Specifically, we have provided a link budget analysis, deriving the average received SNR as a function of the UAV's position in the 3D space. Moreover, we have derived closed-form expressions for both the OP and the AOD which can be used to evaluate the system's reliability and latency.

APPENDIX A PROOF OF PROPOSITION 1

Let the UAV be in an arbitrary location (r, θ, ϕ) in the 3D space. The path loss of the UAV-RIS link $l_1 = \frac{A}{E_f}$ where $E_f = \pi\alpha\beta$ is the radiation footprint area and α and β are its radii. The ellipse's major axis can be calculated by utilizing the law of cosines as

$$\alpha = (CD) - (ED) = \left| \frac{r \sin(\phi) \sin(\theta)}{\tan(\phi)} - \frac{r \sin(\phi) \sin(\theta)}{\tan(\phi' + \frac{\xi}{2})} \right|. \quad (15)$$

In (15), we need to determine the angle ϕ' which can be calculated numerically by equalizing the line segments (CE) and (FC) as shown in Fig. 1 and considering that $g(\phi') = (CE) - (FC)$. As shown in Fig. 2, the points of the major axis have elevation angle θ and azimuth angle 0 or π since they are located at the plane $y = 0$. Furthermore, the first coordinate of the aiming point is calculated as $(CD) - (KD)$ as shown in Fig. 1, thus $K \equiv \left(|r \sin(\theta) \cos(\phi) - \frac{r \sin(\theta) \sin(\phi)}{\tan(\phi')}|, \theta, \varsigma \right)$ with $\varsigma = 0$ if $\phi \leq \frac{\pi}{2}$ or $\varsigma = \pi$ if $\phi > \frac{\pi}{2}$. Moreover, the minor axis coincides with the base of the isosceles triangle with opposite angle ξ and height r , thus it can be expressed as

$$\beta = r \tan\left(\frac{\xi}{2}\right), \quad (16)$$

After the calculation of the radii, we can calculate the radiation footprint area E_f and the path loss of the UAV-RIS link l_1 which concludes the proof.

APPENDIX B PROOF OF PROPOSITION 2

Due to the directional transmission, the incident power at the RIS is equal to the percentage of the transmit power that lays inside the RIS. Utilizing the lines that define the RIS sides and the equation of a rotated ellipse which is given by

$$\frac{(x \sin(\theta) + y \cos(\theta))^2}{\alpha^2(\xi)} + \frac{(x \sin(\theta) - y \cos(\theta))^2}{\beta^2(\xi)} = 1, \quad (17)$$

we can determine the intersection points x_1, x_2, z_1 and z_2 . Considering Fig. 2 and the different cases regarding the intersection points of the radiation footprint with the RIS sides, the corresponding arc areas and triangles are calculated. Next, the area of the footprint that lies outside of the RIS is calculated which enables the derivation of M . Since the UAV always hovers in a location where a large number of reflecting elements is illuminated, i.e., $M \gg 1$, according to the central limit theorem, H converges to a Gaussian distributed random variable \tilde{H} .

APPENDIX C PROOF OF COROLLARY 2

The AOD is defined as [10]

$$A(z) = \frac{\mathcal{P}_o(z)}{L(z)}. \quad (18)$$

For an arbitrary stationary differentiable random process $x(t)$, the LCR is given by [10]

$$L(z) = \int_{-\infty}^{\infty} |\dot{x}| f_{X,\dot{X}}(z, \dot{x}) d\dot{x}, \quad (19)$$

where \dot{x} is the first derivative of x with respect to time and $f_{X,\dot{X}}(z, \dot{x})$ is the joint probability density function (PDF) of $x(t)$ and $\dot{x}(t)$ at time t . Considering that H is a sum of M RVs following the Nakagami- m distribution, the LCR can be expressed as [11]

$$L(z) = f_H(z) \frac{\sigma_{\dot{x}}}{\sqrt{2\pi}}, \quad (20)$$

where $\sigma_{\dot{x}} = \pi f_D \sqrt{\frac{M\Omega}{m}}$ and $f_H(z)$ denotes the PDF of H . Approximating $f_H(z)$ with the PDF of \tilde{H} which is given by

$$f_{\tilde{H}}(z) = \frac{1}{\sqrt{2\pi \text{Var}[\tilde{H}]}} e^{-\frac{(z - \mathbb{E}[\tilde{H}])^2}{2\text{Var}[\tilde{H}]}} , \quad (21)$$

(14) is derived, which completes the proof.

REFERENCES

- [1] P. S. Bithas, V. Nikolaidis, A. G. Kanatas, and G. K. Karagiannidis, "UAV-to-Ground Communications: Channel Modeling and UAV Selection," *IEEE Trans. Wireless Commun.*, vol. 68, no. 8, pp. 5135–5144, Aug. 2020.
- [2] S. A. Tegos, D. Tyrovolas, P. D. Diamantoulakis, and G. K. Karagiannidis, "On the Distribution of the Sum of Double-Nakagami-m Random Vectors and Application in Randomly Reconfigurable Surfaces," 2021. [Online]. Available: <https://arxiv.org/abs/2102.05591>
- [3] S. Li, B. Duo, X. Yuan, Y.-C. Liang, and M. Di Renzo, "Reconfigurable Intelligent Surface Assisted UAV Communication: Joint Trajectory Design and Passive Beamforming," *IEEE Wireless Commun. Lett.*, vol. 9, no. 5, pp. 716–720, May 2020.
- [4] K. Ntontin, A.-A. A. Boulogeorgos, D. Selimis, F. Lazarakis, A. Alexiou, and S. Chatzinotas, "Reconfigurable Intelligent Surface Optimal Placement in Millimeter-Wave Networks," 2021. [Online]. Available: <https://arxiv.org/abs/2011.09949>
- [5] C. B. Issaid and M.-S. Alouini, "Level Crossing Rate and Average Outage Duration of Free Space Optical Links," *IEEE Trans. Commun.*, vol. 67, no. 9, pp. 6234–6242, Sep. 2019.
- [6] D. Hilbert and S. Cohn-Vossen, "Geometry and the imagination," New York: Chelsea Publishing Company, 1952.
- [7] Q. Wu and R. Zhang, "Intelligent Reflecting Surface Enhanced Wireless Network via Joint Active and Passive Beamforming," *IEEE Trans. Wireless Commun.*, vol. 18, no. 11, pp. 5394–5409, Nov. 2019.
- [8] G. B. Hughes and M. Chraibi, "Calculating ellipse overlap areas," *Comput. Visual. Sci.*, vol. 15, no. 5, pp. 291–301, Oct. 2012.
- [9] H. Shakhatreh, A. Khreichah, N. S. Othman, and A. Sawalmeh, "Maximizing indoor wireless coverage using UAVs equipped with directional antennas," in *2017 IEEE 13th Malaysia International Conference on Communications (MICC)*, Nov. 2017, pp. 175–180.
- [10] M. D. Yacoub, J. E. V. Bautista, and L. Guerra de Rezende Guedes, "On higher order statistics of the Nakagami- m distribution," *IEEE Trans. Veh. Technol.*, vol. 48, no. 3, pp. 790–794, May 1999.
- [11] C.-D. Iskander and P. Takis Mathiopoulos, "Analytical level crossing rates and average fade durations for diversity techniques in Nakagami fading channels," *IEEE Trans. Commun.*, vol. 50, no. 8, pp. 1301–1309, Aug. 2002.